

Formation of Secondary Pollutants During Long-Range Transport and Its Contribution to Air Quality in East Asia

HIROMASA UEDA¹ and GREGORY R. CARMICHAEL²

(Manuscript received 12 June 1994, in final form 15 March 1995)

ABSTRACT

The relationship between secondary pollutants and their formation during long-range transport (LRT) and its contribution to air quality in East Asia were investigated through field observations and numerical simulations. At first, it was found that the tropospheric ozone level in this area was highest in the world with maximum values occurring in the spring. This was suggested to have been caused by two mechanisms: the stratospheric ozone intrusion into the troposphere, and the regional-scale LRT of anthropogenic pollutants and the tropospheric ozone formation caused by them. This was found to be associated with yellow sand events and to cause a simultaneous increase in spm and ozone concentrations. The elevated ozone concentration was predicted well by an Eulerian transport / chemistry / deposition model (STEM-II model, Carmichael *et al.*, 1986), which quantitatively suggested the important role of the latter mechanism. In addition, a clear insight into chemical processes during LRT was presented, based upon the concentration changes of secondary pollutants and radicals (OH and RO₂) along the route of LRT in central Japan.

(Key words: Long range transport, Photochemical reaction, Tropospheric ozone, Regional-scale air pollution, East Asia)

1. INTRODUCTION

The prediction and management of air quality is gaining increasing importance around the world. In fact, its significance can be expected to increase in future as there is growing concern about the effects of air pollution on the earth's ecosystems.

¹ Research Institute for Applied Mechanics, Kyushu University, Kasuga Park 2, Kasuga, Fukuoka 816, Japan

² Department of Chemical and Biochemical Engineering, University of Iowa, Iowa City, Iowa 52242-1219, U.S.A.

Air pollutants are transported over long distances and across political boundaries. Through the mechanisms of long-range transport (LRT), chemical species emitted into the atmosphere from urban and industrial centers are distributed over large regions and transformed into various kinds of secondary pollutants of high concentrations. As a result, widespread pollution problems, such as regional elevated oxidant levels, acid deposition and visibility impairment occur. The LRT of air pollutants has been widely studied in the past decade, but most of these studies have focused on Europe and North America.

One of the economically fastest growing regions of the world is East Asia where the strong potential for pollution problems can be anticipated, based on the present and projected growth in emissions and the close geographical proximity of many of the major industrial and urban centers (e.g., Tokyo, Seoul, Taipei, Shanghai, Hong Kong). Through LRT processes, pollutants emitted from the various countries are expected to contribute in adverse ways to the air quality of the entire East Asia region.

The present paper focuses on the formation of secondary pollutants during LRT and its contribution to the air quality in East Asia. The relationship between various secondary pollutants is also discussed. Although the results shown here are mainly quoted from a series of previous works of these authors, their review, together with new analysis on the behavior of important radicals, such as OH and RO₂ radicals, makes it possible to better understand the overall atmospheric reaction process during LRT and the air quality in East Asia. At first, the formation of secondary pollutants during LRT and the relationship between them, based upon results of a systematic field observation in central Japan as well as its numerical simulation, are discussed. Then air pollution associated with the yellow sand events, a good indicator of the regional-scale LRT is studied. Finally, the characteristics of air quality in East Asia are assessed.

2. VARIATION OF AIR QUALITY DURING LONG-RANGE TRANSPORT

A comprehensive field observation of the mesoscale transport of pollutants was conducted in central Japan (Kurita *et al.*, 1985, 1990) in the summers of 1983, 84 and 1986. Gaseous and particulate pollutants together with meteorological parameters were observed at 16 sites along the path of the polluted air mass from the Tokyo metropolitan area (highly industrialized and populated area) to the Central Mountainous Region (Figure 1). Aircraft measurements were also conducted along the LRT path. The measured pollutants included NO, NO₂, SO₂, O₃, CO, HNO₃, HCl, nitrate and sulfate as well as the components of hydrocarbons, aldehydes, fatty acids and mono- and di-carboxylic acids.

A series of numerical simulations were also conducted using an advanced Eulerian combined transport/chemistry/deposition model (referred to as the STEM-II model, Carmichael *et al.*, 1986) to obtain the concentration changes in primary and secondary pollutants and those of radicals and dry and wet depositions along the transport path (Chang *et al.*, 1989 a,b, 1990). This model utilized the updated reaction mechanism of Atkinson (1990), which included 112 chemical reactions and 53 chemical species. Of these species, 33 long-lived species are advected, while the remaining 20 short-lived ones, such as free radicals, were modeled using the pseudo-steady state approximation. In addition to gas phase chemistry, the equilibrium relationship for the HNO₃-NH₃-NH₄NO₃ system was included in the analysis.

The spatial and temporal variations for emission distributions, meteorological data, initial and boundary conditions were given for the model calculations. Meteorological input field and initial surface concentrations were obtained from the observed data. At the top boundary, the total inflow was calculated by equating the concentration of the boundary grid

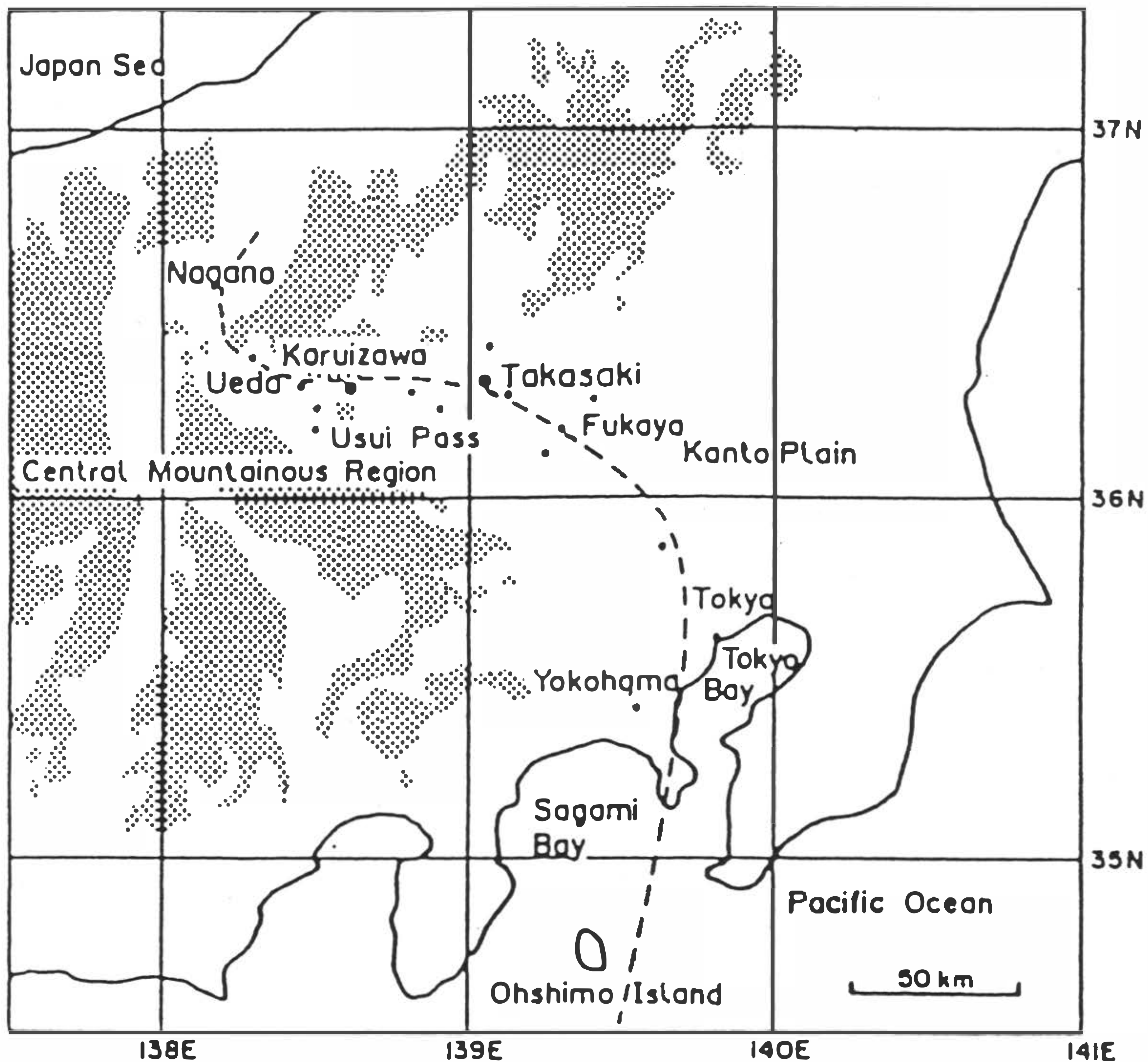


Fig. 1. Geographical features and sampling sites. Dashed line represents the actual route of the long-range transport. Land higher than 1000 m MSL is denoted by the stippled areas. ●: observation sites of meteorology and/or chemistry, ●: sampling sites of airborne aerosols.

point with that of the surrounding exterior, under the assumption that the concentration level there was relatively low. At the side boundaries, the inflow conditions were determined by running a one-dimensional STEM-II model under appropriate surface emission conditions. The boundary conditions were updated every hour. Complete details of the simulation were described in Chang *et al.* (1989).

The transport mechanism for this particular situation is different from that caused by gradient winds. The latter type of LRT is usually accompanied by a moving high pressure system, the typical examples of which are observed in North America and Europe. In North America, air pollution from the central Midwest is transported more than 1000 km to the upper Midwest and to the Great Plains in the central U.S. (Hall *et al.* 1973). In Europe, photochemical ozone is transported from the industrialized and populated Continent to remote sites in the southern U.K. and Ireland, covering long distances of up to 1000 km in several days.

LRT in central Japan is mainly caused by a combination of local winds. The key components include land/sea breezes, mountain valley winds, plain plateau wind, steady onshore wind and steady plain wind which are merged into a large wind system by subsidence inversion under a synoptic-scale high pressure system. Thus this type of LRT occurs during periods of light gradient winds. Similar LRT has been found on the East Coast of the U.S. by Carroll and Baskett (1979) and Edinger *et al.* (1972), but in this type of LRT, pollutants

are transported deeply into the center of the mountainous regions. A typical wind system and transport path of pollutants are shown in Figure 1. Such clear summer days on which this type of LRT occurs also correspond to periods when the photochemical processes (and subsequent secondary pollutant formation) are most active. As a result of such transport and the favorable photochemical conditions, high concentrations of photochemical oxidants and other secondary pollutants are observed over the inland regions on clear summer days. Moreover, these high concentrations due to secondary pollutants, transported inland via the LRT mechanism, usually occur in the mountainous areas in the late evening or sometime around midnight (referred to as night-time smog).

The observed distributions along the LRT path and their time variations of primary and secondary pollutants, such as of NO, NO₂, SO₂, O₃, CO, HNO₃, HCl, nitrate and sulfate and components of hydrocarbons, were compared with those simulated by the STEM-II model. This model predicted the observed behavior of primary and secondary pollutants well and also gave a good prediction of OH and RO₂ radical concentrations. Thus, since the model results provide a clearer and more comprehensive explanation about the behavior of secondary pollutants, mainly these results are used in the following discussion.

2.1 Oxidants

Ground-level O₃ concentrations at the seven observation sites along the transport path (Figure 1) are presented in Figure 2. The O₃ values in the large emission source region (Yokohama and Tokyo) show a typical diurnal variation usually found in polluted areas. A rather low maximum appears at around noon, reflecting higher NO_x emissions. At Urawa, about 25 km away from downtown Tokyo, the O₃ concentrations increase to about 120 ppb. The transport of the polluted air mass can clearly be seen in the O₃ values at Takasaki and Karuizawa. The peak O₃ values increase further, and when the air mass is transported over the mountain pass, it attains a maximum value greater than 150 ppb at about sunset. In this scenario, Karuizawa is the forefront observation site under the large-scale wind field from the Pacific Ocean, while Nagano and Ueda are in the wind regime from the Japan Sea with small emission sources.

Other important components of oxidants are PAN and H₂O₂ although their concentration measurements were not made. Figure 3 shows their predicted time variations. The behavior of PAN is similar to that of O₃ with its maximum concentration being about 1/20 of the maximum O₃ value. In addition, a significant concentration of PAN is predicted in the mountainous region. H₂O₂ is produced more slowly, but the maximum concentration attains 5 ppb.

The region of highest oxidant levels (ozone and H₂O₂) corresponds to regions of environmental damage. Tree growth data in the forests of the Kanto Plain and Central Mountainous Region of Japan were collected and analyzed. Forest damage was found throughout this study region, with the region of highest damage extending along a curved path from Tokyo into the Ueda and Nagano Basins in the Central Mountainous Region. This region corresponds to that which receives the highest oxidant levels. Although this data do not directly show a cause and effect relation, there is growing evidence relating high levels of secondary pollutants to such forest damage.

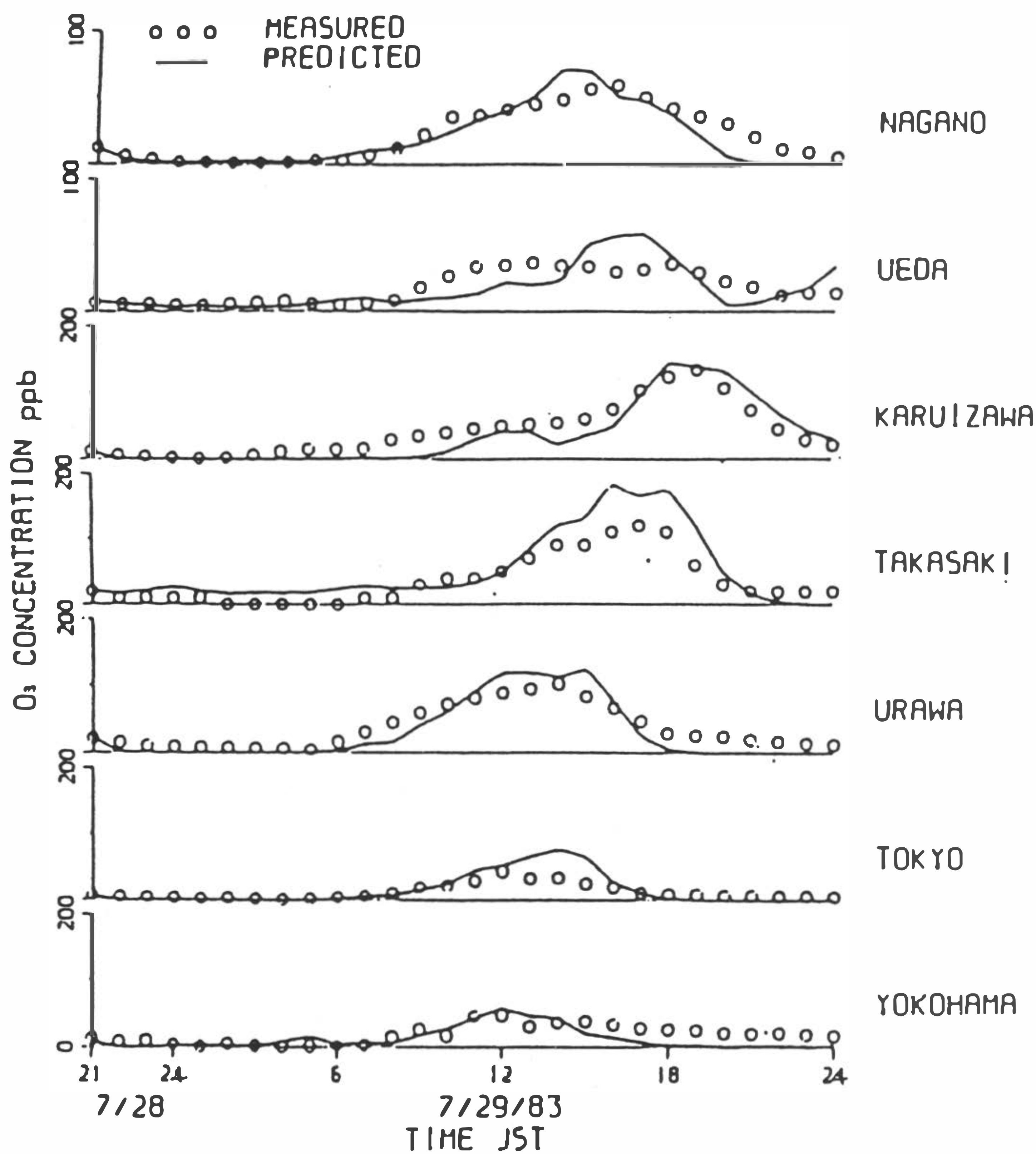


Fig. 2. Comparison of measured and predicted values of O_3 .

2.2 OH and RO_2 Radicals

OH and RO_2 radicals produced in photochemical reactions play key roles in the oxidation of NO_x , SO_x , hydrocarbons and other pollutants during LRT. From the observed destruction rates of hydrocarbon components and/or O_3 formation rates, the OH radical concentration in the polluted air mass is estimated and presented in Figure 4 (Satsumabayashi *et al.*, 1992). OH is found to increase from 0.5×10^{-7} ppm in the morning to a maximum of 8.0×10^{-7} ppm at midday and then to decrease, estimates which are consistent with STEM-II model predictions. In addition, the morning values are supported by the 1.5×10^{-7} ppm estimated from the NO_x - NO_3^- conversion rate, $14.7\%h^{-1}$ in this observation. They also compare well with the 1.0×10^{-7} ppm estimated in Los Angeles (Calvert, 1976) and the 0.2 - 2×10^{-7} ppm observed by Hewitt and Harrison (1985) during the daytime in an urban area.

RO_2 radical concentration, $[RO_2]$, was also estimated by assuming the photostationary steady state in the following photochemical cycle:



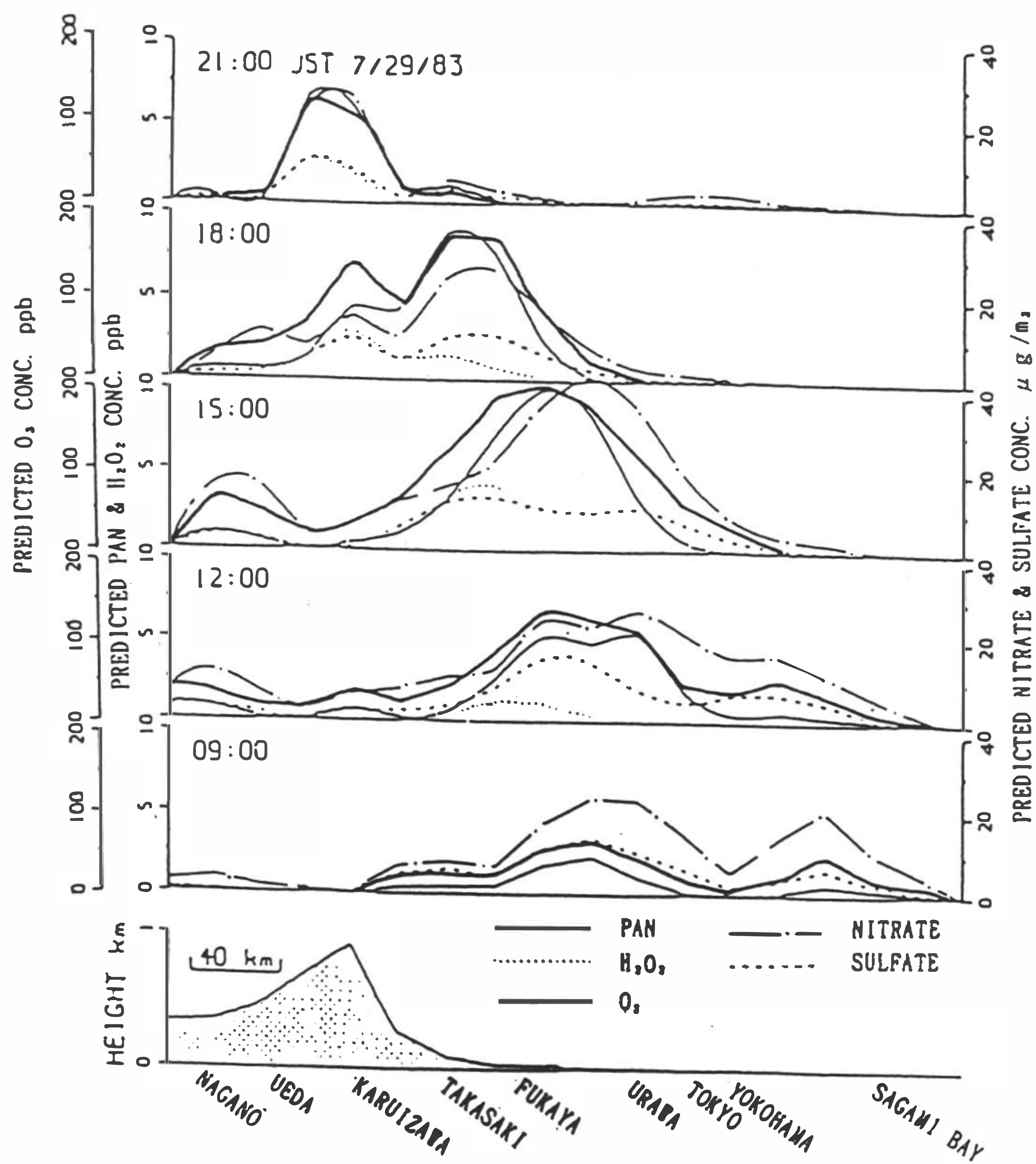


Fig. 3. The surface concentrations of selected species as a function of location and time.

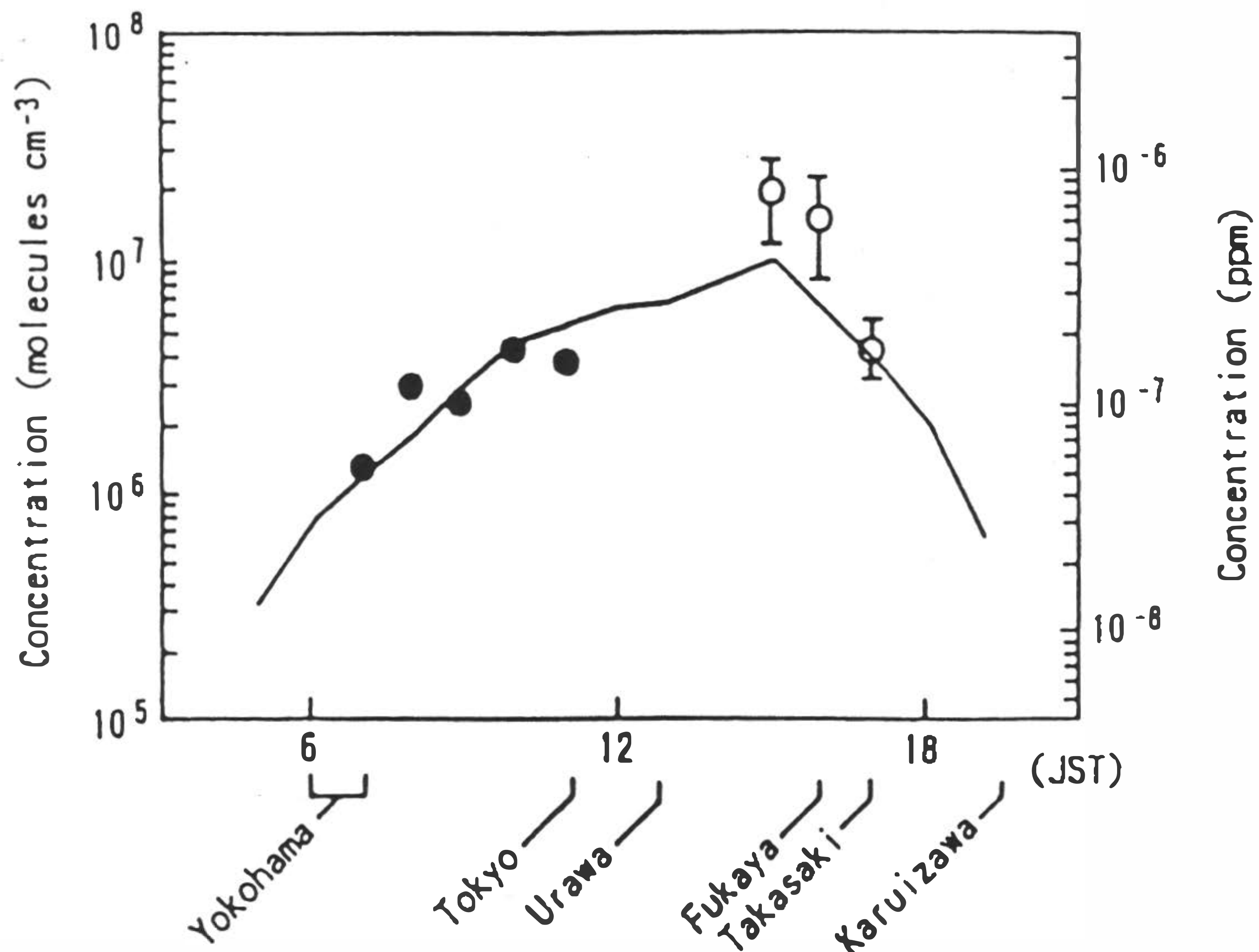


Fig. 4. OH radical concentrations along the trajectory of Figure 1 (29 July 1983). o: Mean and one standard deviation taken from time variations of ratios between hydrocarbon components, ●: derived from rates of ozone formation, k_e and nonmethane organic matter concentrations, —: model prediction.

The estimated $[RO_2]$ at Yokohama, Tokyo and Urawa is presented in Figure 5 (Satsumabayashi *et al.*, 1993). It increases in the daytime, with a maximum of 1.2×10^{-4} ppm at 1200 LST but decreases thereafter by an order of two magnitude. The average value over the period 900-1200 LST was 0.8×10^{-4} ppm.

These estimated values compare well with the values from the STEM-II model. The predicted $[RO_2]$ ranges from 0.1×10^{-4} to 1.0×10^{-4} ppm as the air mass moves from the Tokyo metropolitan area into the Central Mountainous Region. Approximately 60%, 20% and 20% of the total $[RO_2]$ was due to HO_2 , CH_3O_2 and other organic radicals, respectively.

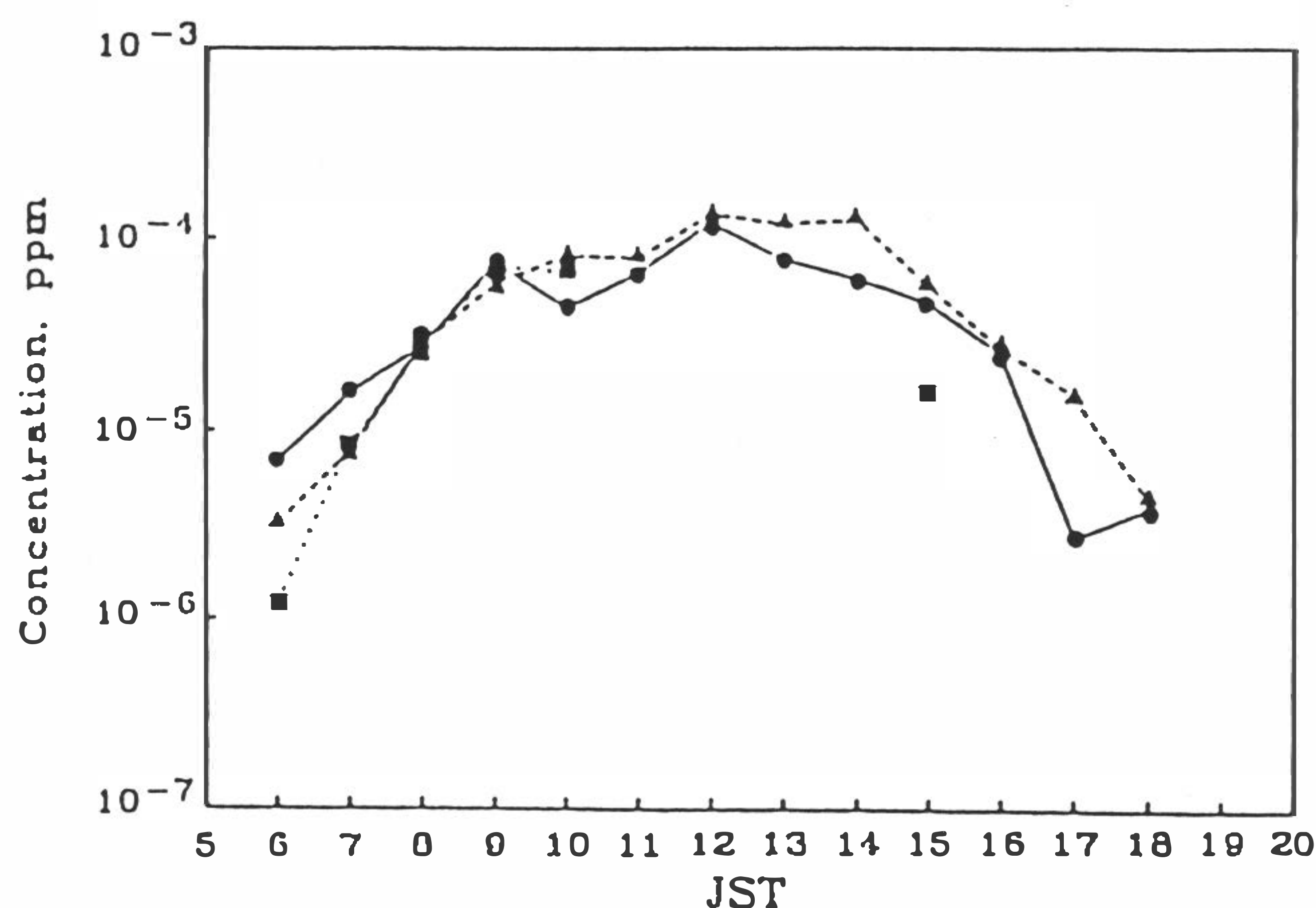


Fig. 5. Diurnal variation of the estimated RO_2 radical concentration (29 July 1983). o—o: Yokohama, Δ - - Δ : Tokyo, \blacksquare \blacksquare : Urawa.

2.3 Nitrate, Sulfate and Other Inorganic Aerosols

Gaseous nitric acid, aerosol NO_3^- and PAN are the major end products of NO_x oxidation which proceeded almost simultaneously with the formation of O_x , with almost all of the HNO_3 and NO_3^- being formed during the period when O_x concentration was at its maximum. The conversion rate averaged over this range was $14.7\%h^{-1}$ (Sasaki *et al.*, 1985).

In contrast, SO_2 oxidation proceeded slowly. The conversion rate was $3.7\%h^{-1}$, or about a quarter of that for NO_x . These results are consistent with those from Calvert and Stockwell (1983). The predicted behavior of SO_2 , SO_4^{2-} , NO and NO_2 as they were transported inland, was in good agreement with the observed surface concentration. However, the HNO_3 concentrations were greatly overpredicted, necessitating some additional loss mechanism for the observed total value of NO_x and total nitrate. The prediction was greatly improved by the inclusion of a loss mechanism through deposition on dust particles as suggested by Kelly (1987).

Nitrate aerosol formation when the air mass entered the mountainous region was explained well by an equilibrium model (Stelson and Seinfeld, 1982 a,b; Chang *et al.*, 1986). This means that at high temperature and low humidity, most of the nitrate was in gaseous HNO_3 , whereas at lower temperatures, the nitrate was in solid and aqueous particles at low and high humidities, respectively. The SO_4^{2-} formation was predicted well with the inclusion of heterogeneous reactions. It existed in the form of aerosol. At an elevated remote

site (Karuizawa, about 1000 m MSL), the aerosol ion balance between anion (SO_4^{2-} , NO_3^- and Cl^-) and cation (NH_4^+ , Na^+ , Ca^{2+} , K^+ and Mg^{2+}) was excellent with a correlation coefficient of 0.996, during local pollution situations (i.e. at relatively low pollution levels). However, during LRT, the ion balance shifted toward the anion side for which the presence of H^+ in the form of H_2SO_4 mist or NH_4HSO_4 is suggested as having been responsible (Sasaki *et al.*, 1988). A much larger imbalance at the Happo Ridge (1840 m MSL) in which the cation was about 50% of the anion, is conjectured to have been caused by very low concentrations of gaseous NH_3 .

The fates of SO_x and NO_x compounds during LRT are summarized in their respective budget diagrams (Figure 6). More than one half of the NO_x emission was removed in one day, mainly owing to a large dry deposition velocity of gaseous HNO_3 . In contrast, only 20% of the SO_2 emitted was removed by dry deposition, and consequently, sulfate remained in the atmosphere for a longer time in the form of aerosol. According to Chang *et al.* (1990), the major removal mechanism for the SO_4^{2-} aerosol under these conditions is wet removal.

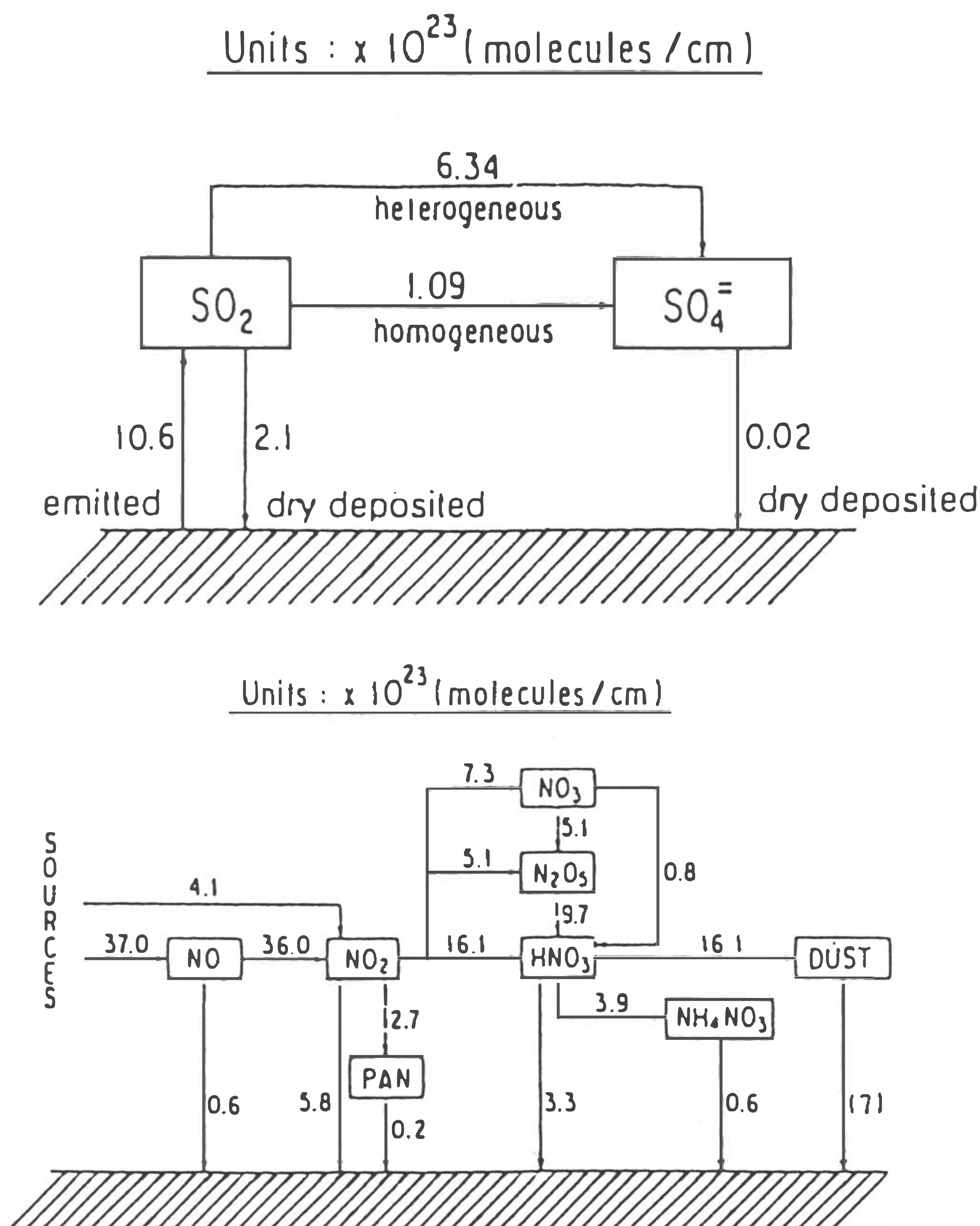


Fig. 6. Budgets of SO_x and NO_x species.

2.4 Hydrocarbons, Aldehydes and Organic Aerosols

A large amount of hydrocarbons is emitted in the Tokyo metropolitan area, of which paraffin is the most abundant, followed by aromatics and olefin. They are decomposed to oxygenated organic matters, such as aldehydes and organic acids in the photochemical re-

actions during LRT, and some of their components are condensed to form organic aerosols (Satsumabayashi *et al.*, 1989, 1990). On the basis of the gas-phase chemical reaction mechanism (Carmichael *et al.*, 1986; Atkinson, 1990) and the estimated OH and RO₂ radical concentrations and observed O₃ as well as other component concentrations, the amount of hydrocarbon decomposition was estimated. It was found that toluene was largest, followed by ethylene, n-butane, isopentane, n-pentane and m-xylene. Ethane, propane, acetylene and benzene contributions were small in spite of their high concentrations (Satsumabayashi *et al.*, 1990).

As most of the aldehydes and fatty acids, in fact more than 50%, were estimated to have been produced by photo-oxidation, these concentrations increased in the daytime and decreased at night. The diurnal variation patterns of these species were very similar to those of O₃. The observed production rates of formaldehyde, acetaldehyde and formic acid were 4.1, 1.1 and 0.5 ppb h⁻¹, respectively. These values compare very well with the model predictions. However, the prediction of acetic acid production rate was initially too low but was improved to the observed value of 0.4 ppb h⁻¹ by having the production mechanism included as suggested by Moortgat *et al.* (1989) and Madronich *et al.* (1990).

Of the airborne particulates, more than half were carbon aerosols, i.e., organic carbon OC and elementary carbon EC (Figure 7). The OC concentration increased significantly during LRT. In particular, the diurnal variation pattern of polar organic carbon (POC) concentration agreed well with that of O₃, comprising 64% of OC when the air mass arrived at Takasaki. The fraction produced by photochemical reactions was estimated to be 61% of POC, 39% of OC and 14% of total aerosol in weight. Of the detected components, dicarboxylic acids (C₂-C₁₀) were the most abundant during the daytime, but phthalates (dibutyl and bis (2-ethylhexyl)), C₂₁-C₃₂ n-alkanes, pinon-aldehyde and fatty acids (C₁₀-C₂₆) were also abundant aerosol species. Of the dicarboxylic acids, succinic acid was the most abundant, followed by phthalic acid and maronic acid, with their concentrations ranging from 20 to 130 ng m⁻³. Oxalic acid concentration was low because of its high volatility.

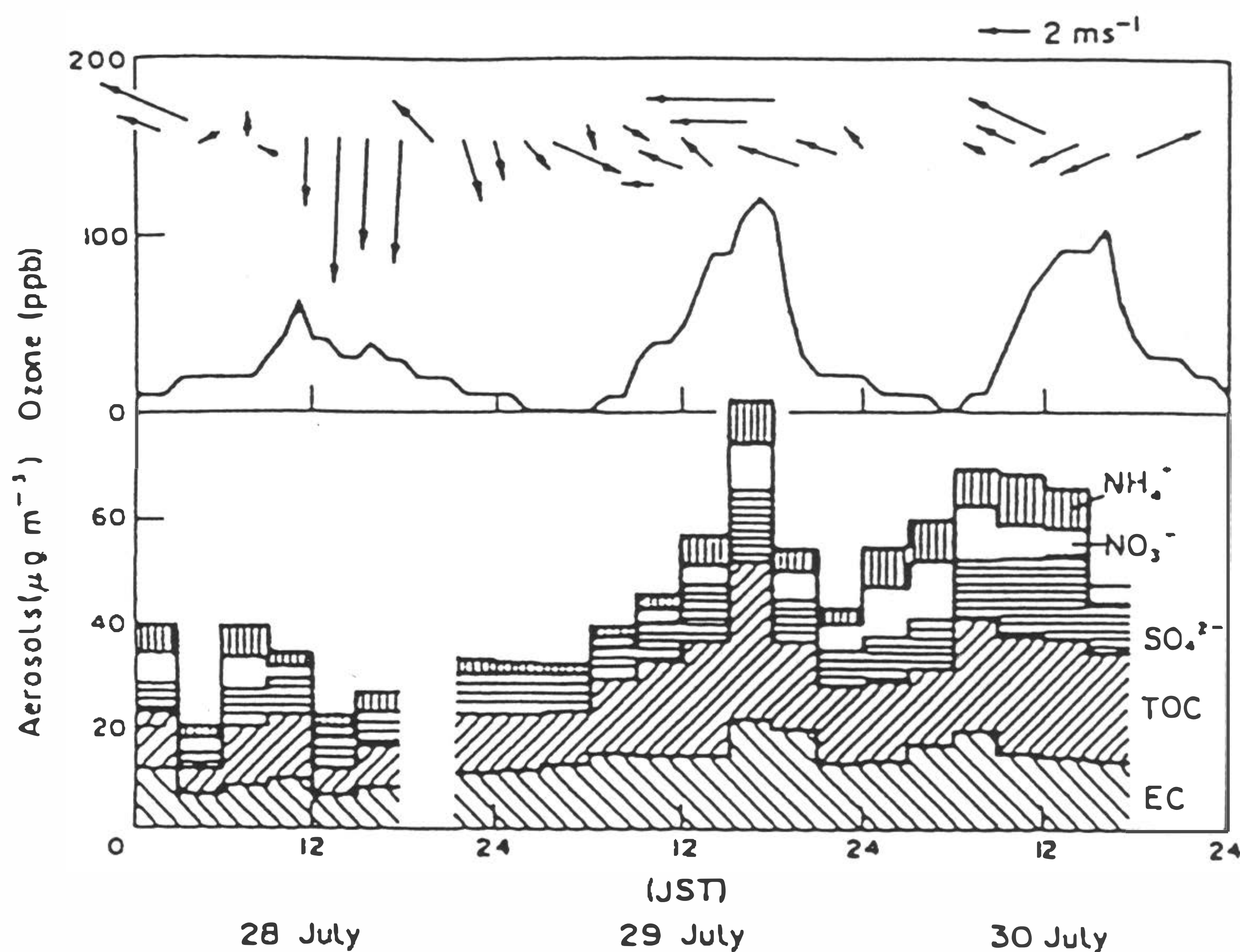


Fig. 7. Diurnal variations of wind vectors at 50 m and aerosol component concentrations at Takasaki in 1983.

Besides the components identified above, the polar unresolved complex mixture (PUCM) and the nonpolar one (NPUCM) were detected through the use of chromatography. They occupied a fraction about 10 times larger, although the detected total fraction, including the PUCM and NPUCM, was 30-50% of the total organic carbon. From the ratio of odd to even carbon number components, more than a half of the n-alkanes was estimated to be anthropogenic. Biogenic compounds were a minor contributor to airborne aerosol since a large part of them, e.g., pinonaldehyde, was considered to have been produced photochemically but to be in its gaseous phase in the daytime. Almost all of dicarboxylic acids and about half of the NPUCM and PUCM were also produced during LRT. Therefore, the secondary components produced during LRT attained 42-53% of the organic compounds detected.

3. LONG-RANGE TRANSPORT OF POLLUTANTS ACCOMPANIED BY YELLOW SAND EVENTS

One of the most prominent features of the air quality in East Asia is airborne dust consisting mainly of soil components, the so-called yellow sand. The dust deposition rate, the highest in the world, is more than $10000 \text{ mg m}^{-2} \text{ yr}^{-1}$ in the entire East Asia and adjoining Pacific Ocean, and area much larger than the Sahara desert, for example. The dust and NH_3 with high concentrations work to neutralize airborne acidic matters and result in the comparatively low acidity of precipitation in the northern part of China, Korea and Japan despite high concentrations of sulfate.

Another air pollutant of interest from the standpoint of LRT is ozone. Recently, Fishman and Larsen (1987) developed a technique to estimate tropospheric ozone using satellite measurements of total and stratospheric ozone. Many important features appear from this analysis. However, the strongest gradients and highest values of integrated tropospheric ozone in each season are found in East Asia, in the area extending from central China out into the central Pacific Ocean. Figure 8 shows the global distribution of tropospheric ozone in the springtime, the time of its peak concentration.

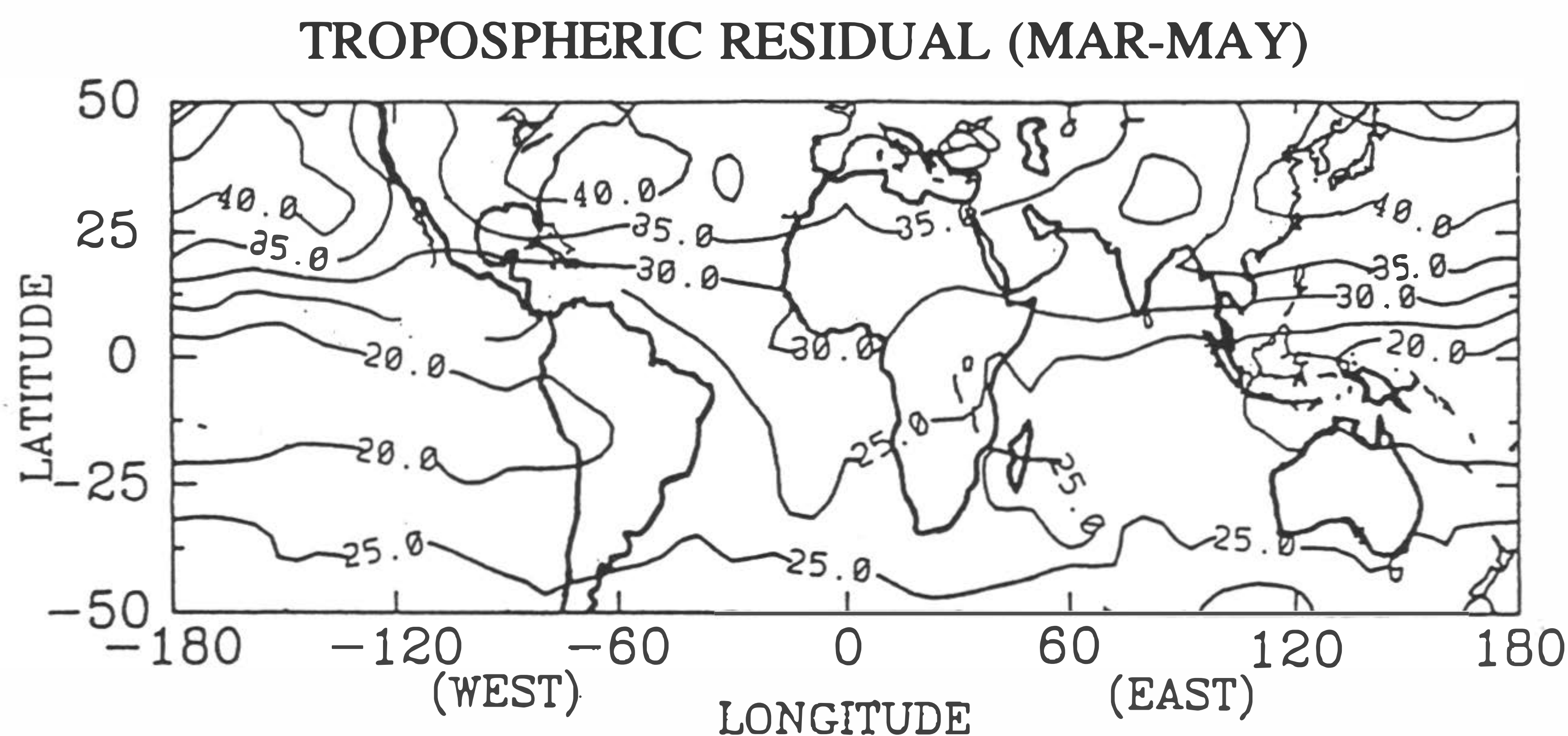


Fig. 8. Global distribution of ozone (March-May, 1987).

Continuous observations of surface ozone concentration have been made since 1985 (Kurita *et al.*, 1989) at elevated remote sites in central Japan (Happo Ridge, 1840 m MSL). The annual variation shows that ozone increases gradually in winter and reaches a significant

peak in April or May. Similar seasonal variations are observed at other remote monitoring stations all over Japan.

The increase in ozone concentration is considered to be caused by two mechanisms, (1) by photochemical reactions of anthropogenic pollutants (Liu *et al.*, 1987; Janach, 1989), and (2) by the intrusion of stratospheric ozone (Wakamatsu *et al.*, 1989). Indeed, the activities of jet stream and high pressure system become most active in the springtime in this region. Both are believed to cause stratospheric ozone intrusion events and to give rise to increases in the tropospheric ozone column. Evidence of ozone intrusion was suggested by a field observation (Wakamatsu *et al.*, 1989) in which stratospheric ozone moved down into the upper troposphere due to the descending flow near the front of the cold arctic air mass and subsequently reached to the surface in a high pressure system. However, the amount of the intruded ozone has not been well quantified.

Ozone concentrations are further increased through LRT and photochemical production from anthropogenic pollutants in the troposphere. In spring, when the ozone concentration increases, the regional-scale LRT of yellow sand occurs frequently and is recognized as a visible dust storm (yellow colored). It is transported eastward from the Chinese deserts and Losses Plains and covers the middle-latitude region of the Pacific Rim.

Air pollution associated with the yellow sand events was investigated at elevated remote sites in central Japan (Kurita *et al.*, 1989). Backtrajectory of the yellow sand, e.g., on 5 May 1985 when a severe dust storm attacked Japan, showed that this sand from the Chinese deserts, passed through the Shantong and Korean Peninsulas and arrived in western and central Japan. This is the typical route of the regional-scale LRT. During this event, concentrations of spm and ozone (Figure 9) increase, this being associated with a significant increase in ozone concentration. Similar simultaneous increases in spm and ozone concentrations occurred in many yellow sand events, suggesting that the LRT of ozone is somehow associated with the yellow sand events, and the high concentration of ozone originates from tropospheric production during LRT.

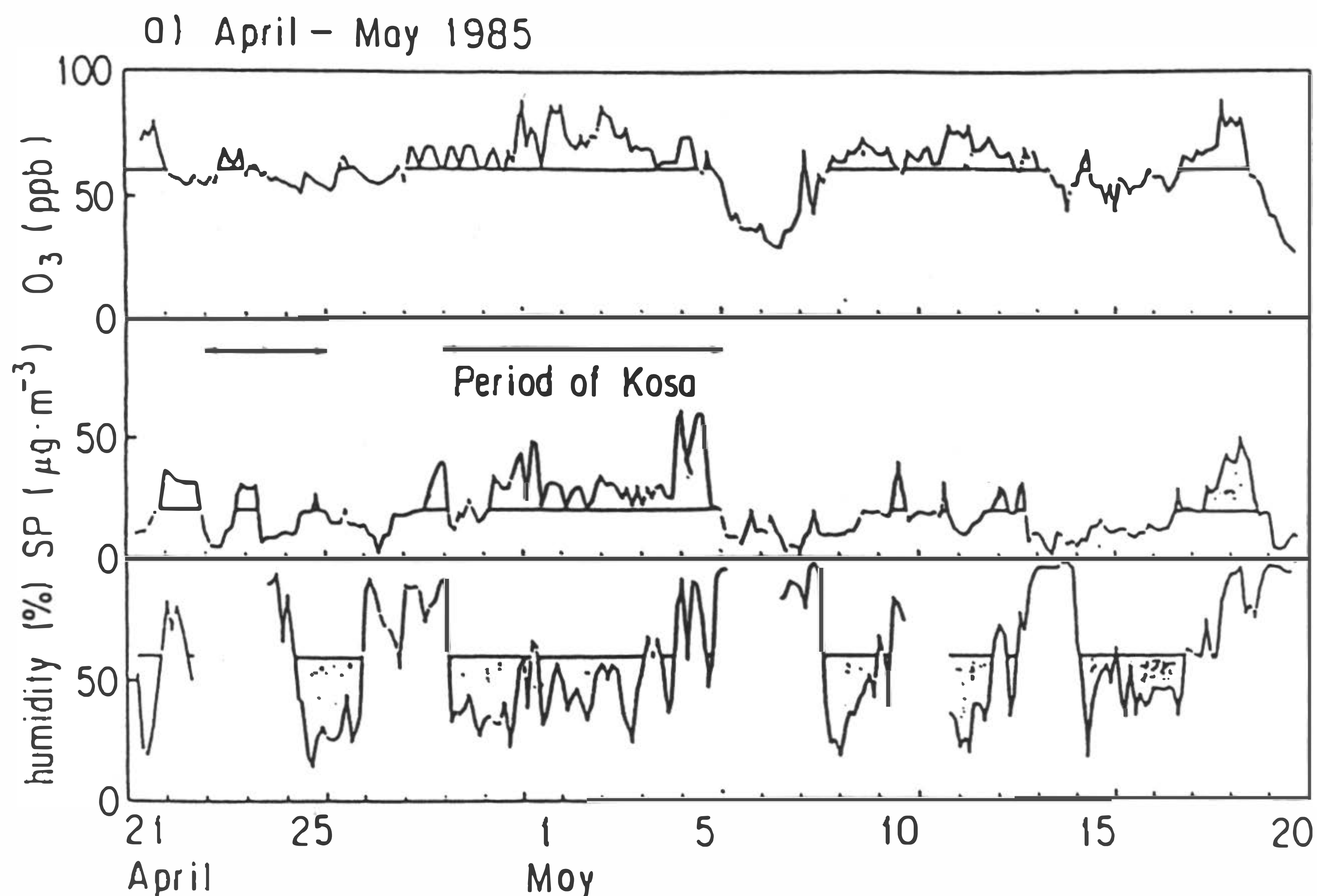


Fig. 9. Diurnal variations of ozone and spm concentrations and relative humidity at Happo ridge during 21 April~20 May, 1985.

In an attempt to quantify the processes leading to elevated ozone levels and to further assess the contribution of photochemical reactions of anthropogenic pollutants, a preliminary numerical simulation was made for this yellow sand event (Kotamarthi *et al.*, 1990). With the emission inventory compiled on the basis of Hameed and Dignon (1988) being used, two-dimensional calculations were performed by the STEM-II model for the transport path described above and for the initial and boundary conditions consisting of uniform distributions with 30 ppb of O₃, 1.4 ppb of methane, 6 ppb of NH₃, 80 ppb of CO and 0.6 ppb of ethane.

The predicted ozone concentration in the air as it originated in Beijing at 1000 LT on the first day was ~30 ppb. By the time this air mass reached the western coast of Korea, the ozone level was 70 ppb. As this air mass passed over the NO_x emission sources of Korea, the ozone levels increased to ~125 ppb. Thereafter, it decreased as the air mass passed over the Japan Sea during night time. The air mass reaching Japan had an ozone concentration of ~80 ppb, which was 20 ppb higher than the Japanese environmental standard. The predicted ozone level agreed well with the observation at the Happo Ridge (Figure 9). Similar results were obtained in recent 3-D simulations (Sunwoo *et al.*, 1992). These facts support the hypothesis that the tropospheric ozone production from anthropogenic pollutants contributes to the elevated ozone concentration associated with the yellow sand events and suggest the important role of the regional-scale LRT in this part of the Pacific Rim.

4. CONCLUDING REMARKS

This paper conclusively discusses the formation of secondary pollutants and their interrelation during long range transport (LRT), through field observations and numerical simulations, the summaries of a series of works conducted by Ueda and Carmichael and the reexamination of previous data in light of new results on free radicals, such as OH and RO₂. Additionally, it investigates the characteristics of air quality and the contribution of long-range transport (LRT) in East Asia. The main conclusions drawn from this article are as follows:

- (1) The tropospheric ozone level in this area is the highest in the world with its maximum value occurring in the spring.
- (2) The springtime increase in ozone concentration at elevated remote sites in Japan was found to be associated with yellow sand events. The simultaneous increase in spm and ozone is evidence of regional-scale LRT. Agreement between the observed elevated ozone concentration and the prediction from the STEM-II suggests, in a quantitative way, the important role of LRT and the tropospheric ozone formation from anthropogenic pollutants. Stratospheric ozone intrusion into the troposphere, as a result of intense activities of jet streams and high pressure systems, is suggested although the actual amount of the intrusion could not be estimated. It is clear that these two mechanisms contribute to a complex air quality and pollutant reaction pattern in the troposphere over East Asia. Moreover, because of the rapid increase in NO_x and hydrocarbon emissions in this area (about 5-10%y⁻¹) as well as the increase in SO_x emissions, regional-scale pollution due to tropospheric ozone is expected to become a serious international problem in the near future.
- (3) A detailed observation of pollutant concentrations in central Japan give a clear insight into the formation of secondary pollutants and radicals (OH and RO₂). At the same time, they strongly support the validity of the numerical model used in this study and yet suggest areas of improvement.

In summary, it is clear that air pollution problems associated with the LRT of pollutants are present throughout Asia. However, the situation may change drastically in the future as a consequence of the accelerated development of fossil fuel systems which are planned in many Asian countries and propelled by the very high economic and population growth rates of this region. The expansion of these energy systems, combined with a major fuel shift to indigenous coal, will undoubtedly result in a significant increase in atmospheric emissions in Asian countries. Substantial portions of these emissions will be transported by winds hundreds to thousands of kilometers away from their sources. In the meantime, many countries are attempting to minimize their own local pollution problems by installing taller factory stacks. Such a policy may contribute in adverse ways to the air quality in larger areas of Asia.

The long-term and regional/local impact of these atmospheric emissions will affect not only the natural environment, but will also have far-reaching implications on the commercial and cultural activities, such as forestry, agriculture and tourism. Furthermore, the abatement costs for air pollution precursors are high. To help quantify and anticipate these environmental issues, it is imperative to develop a better understanding of the mechanisms of the LRT of pollutants in Asia.

REFERENCES

- Atkinson, R. 1990: Gas-phase tropospheric chemistry of organic compounds - a review. *Atmos. Environ.*, **24A**, 1-41.
- Calvert, J. G. 1976 : Test of the theory of ozone generation in Los Angeles atmosphere. *Environ. Sci. Technol.*, **10**, 256- 262.
- Calvert, J. G., and W. R. Stockwell, 1983: in Acid Precipitation Series. **3**, 1-62, Butter worth, Boston.
- Carmichael, G. R., L. K. Peters, and T. Kitada, 1986: A second generation model for regional scale transport/chemistry/deposition. *Atmos. Environ.*, **20**, 173-188.
- Chang, Y. S., G. R. Carmichael, H. Kurita, and H. Ueda, 1986: An investigation of the formation of ambient NH_4NO_3 aerosol. *Atmos. Environ.*, **20**, 1969-1977.
- Chang, Y. S., G. R. Carmichael, H. Kurita, and H. Ueda, 1989a: The transport and formation of photochemical oxidants in central Japan. *Atmos. Environ.*, **23**, 363-393.
- Chang, Y. S., G. R. Carmichael, H. Kurita, and H. Ueda, 1989b: The transport and formation of sulfates and nitrates in central Japan. *Atmos. Environ.*, **23**, 1749-1773.
- Chang, Y. S., B. S. Ravishanker, G. R. Carmichael, H. Kurita, and H. Ueda, 1990: Acid deposition in central Japan. *ibid*, **24A**, 2035-2049.
- Fishman, J., and J. C. Larsen, 1987: Distribution of total ozone and stratospheric ozone in the tropics: Implications for the distribution of tropospheric ozone. *J. Geophys. Res.*, **92**, 6627-6634.
- Fishman, J., C. E. Watson, J. C. Larsen, and J. A. Logan, 1987: Distribution of tropospheric ozone determined from satellite data. *J. Geophys. Res.*, **95**, 3599-3617.
- Janach, W. E. 1989: Surface ozone: Trend details, seasonal variations and interpretation. *J. Geophys. Res.*, **94**, 18289-18295.

- Kotamarthi, V. K., Y. Sunwoo, and G. R. Carmichael, 1990: Proc. NATO/CCMS 18th ITM on Air Pollution Modelling and its Application, Vancouver.
- Kurita, H., K. Sasaki, H. Muroga, H. Ueda, and S. Wakamatsu, 1985: Long range transport of air pollution under light gradient wind conditions. *J. Climate Appl. Meteor.*, **24**, 425-434.
- Kurita, H., H. Ueda, and S. Mitsumoto, 1990: Combination of local wind systems under light gradient wind conditions and its contribution to the long-range transport of air pollutants. *J. Climate Appl. Meteor.*, **29**, 331-348.
- Madronich, S., R. B. Chatfield, J. G. Calvert, G. K. Moortgat, B. Veyret, and R. Lesclaux, 1990: A photochemical origin of acetic acid in the troposphere. *Geophys. Res. Lett.*, **17**, 2361-2364.
- Moortgat, G. K., B. Veyret, and R. Lesclaux, 1989: Kinetics of the reaction of HO₂ with CH₃C(O)O₂ in the temperature range 253-368. *Chem. Phys. Lett.*, **160**, 443-447.
- Sasaki, K., H. Kurita, G. R. Carmichael, Y. S. Chang, K. Murano, and H. Ueda, 1988: Behavior of sulfate, nitrate and other pollutants in the long-range transport of air pollution. *Atmos. Environ.*, **22**, 1302-1308.
- Satsumabayashi, H., H. Kurita, Y. S. Chang, G. R. Carmichael, and H. Ueda, 1992: Diurnal variation of OH radical and hydrocarbons in a polluted air mass during the long range transport in central Japan. *Atmos. Environ.*, **26A**, 2835-2844.
- Satsumabayashi, H., H. Kurita, Y. S. Chang, G. R. Carmichael, and H. Ueda, 1994: Photochemical formations of lower aldehydes and lower fatty acids under long-range transport in central Japan. *Atmos. Environ.*, **29**, 255-266.
- Satsumabayashi, H., H. Kurita, Y. Yokouchi, and H. Ueda, 1989: Photochemical formation of particulate dicarboxylic acids under long-range transport in central Japan. *Atmos. Environ.*, **24A**, 1443-1450.
- Stelson, A. W., and J. H. Seinfeld, 1982a: Relative humidity and temperature dependence of the ammonium nitrate dissociation constant. *Atmos. Environ.*, **16**, 983-992.
- Stelson, A. W., and J. H. Seinfeld, 1982b: Relative humidity and PH dependence of the vapor pressure of ammonium nitrate-nitric acid solutions at 25°C. *Atmos. Environ.*, **16**, 993-1000.
- Stockwell W. R., and J. G. Calvert, 1983: The mechanism of NO₃ and HONO formation in the night-time chemistry of the urban atmosphere. *J. Geophys. Res.*, **88**, 6673-6682.
- Trainer, M., E. J. Williams, D. D. Parrish, and H. H. Westberg, 1987: Model and observations of the impact of natural hydrocarbons on rural ozone. *Nature*, **329**, p.705.
- Wakamatsu S., I. Uno, H. Ueda, K. Uehara, and H. Tateishi, 1989: Observation study of stratospheric ozone intrusions into the lower troposphere. *Atmos. Environ.*, **23**, 1815-1826.